TISSUE ENGINEERING: Part A
Volume 21, Numbers 13 and 14, 2015
© Mary Ann Liebert, Inc.
DOI: 10.1089/ten.tea.2014.0489

Delivery of Phenamil Enhances BMP-2-Induced Osteogenic Differentiation of Adipose-Derived Stem Cells and Bone Formation in Calvarial Defects

Jiabing Fan, MD, PhD,[1] Choong Sung Im,[1] Zhong-Kai Cui, PhD,[1] Mian Guo, MD, PhD,[2] Olga Bezouglaia, BS,[3] Armita Fartash, BS,[3] Ju-Yeon Lee, BS,[1] John Nguyen, BS,[1] Benjamin M. Wu, DDS, PhD,[4] Tara Aghaloo, DDS, MD, PhD,[3,*] and Min Lee, PhD[1,4,*]

Bone morphogenetic proteins (BMPs) have been widely used for bone repair in the craniofacial region. However, its high dose requirement in clinical applications revealed adverse effects and inefficient bone formation, along with high cost. Here, we report a novel osteoinductive strategy to effectively complement the osteogenic activity of BMP-2 using phenamil, a small molecule that can induce osteogenic differentiation via stimulation of BMP signaling. Treatment of adipose-derived stem cells (ASCs) with BMP-2 in combination with phenamil significantly promoted the *in vitro* osteogenic differentiation of ASCs. The efficacy of the combination strategy of phenamil + BMP-2 was further confirmed in a mouse calvarial defect model using scaffolds consisting of poly(lactic-co-glycolic acid) and apatite layer on their surfaces designed to slowly release phenamil and BMP-2. Six weeks after implantation, the scaffolds treated with phenamil + BMP-2 significantly promoted mouse calvarial regeneration as demonstrated by micro-computerized tomography and histology, compared with the groups treated with phenamil or BMP-2 alone. Moreover, the combination treatment reduced the BMP-2 dose without compromising calvarial healing efficacy. These results suggest promising complementary therapeutic strategies for bone repair in more efficient and cost-effective manners.

Introduction

Current clinical approaches to reconstruct bone remain a major healthcare challenge especially in the craniofacial complex.[1] Although autologous bone grafts have been considered the gold standard for craniofacial reconstruction, they are limited by availability and donor site morbidity and variations in their osteogenic potential.[2,3] Bone morphogenetic protein-2 (BMP-2) is a potent osteoinductive factor that has been extensively used for the treatment of many bone fractures and bone defects.[4] However, supra-physiological milligram-level doses of BMP-2 are required for effective bone repair in clinical practice. Unfortunately, along with high cost, application of such high doses has revealed numerous side effects, such as vertebral osteolysis with cyst formation and life-threatening inflammatory cervical swelling, which have been well documented.[5–8] Thus, there is a need to develop alternative osteoinductive molecular strategies that can effectively complement BMP activity to maximize biological efficiency while reducing BMP dose requirement.

One alternative approach is to deliver small molecule compounds targeting osteoblast differentiation that can synergistically promote bone formation with BMPs. Small molecule compounds are advantageous over growth factor proteins due to their relative low cost, easy synthesis and handling, rapid membrane penetration, and cellular activation.[9] Several small molecules, such as statins and immunosuppressants (e.g., FK506, cyclosporine A), have been shown to induce osteogenic differentiation *in vitro* and bone formation *in vivo*.[10–13] In particular, phenamil is a derivative of the FDA-approved diuretic amiloride, and it has been found to be a strong activator of BMP signaling.[14] These pro-osteogenic effects are thought to be mediated by induction of tribbles homolog 3 (Trb3) that stabilizes Smads and potentiates BMP signaling.[14,15] Recent studies have

[1]Division of Advanced Prosthodontics, UCLA School of Dentistry, Los Angeles, California.
[2]Department of Neurosurgery, the 2nd Affiliated Hospital of Harbin Medical University, Harbin, China.
[3]Division of Diagnostic and Surgical Sciences, UCLA School of Dentistry, Los Angeles, California.
[4]Department of Bioengineering, University of California, Los Angeles, California.
*Co-senior authors.

shown that phenamil induced osteogenesis in human dental pulp cells and mouse bone marrow stromal or preosteoblastic cells.[14,16–19] These results suggest that phenamil can work additively or synergistically with BMP-2 to increase bone regeneration.

Therapeutic efficacy of osteoinductive molecules is affected by delivery kinetics due to their instability and fast degradation, requiring a high therapeutic dose that can lead to unwanted ectopic formation and nontarget toxicity. In prior work, we developed biomimetic apatite layers on the various surfaces of complex three-dimensional (3D) scaffolds, including poly(lactic-co-glycolic acid) (PLGA), tricalcium phosphate, and chitosan (CH), which not only promoted osteogenic activities of progenitor cells but also presented a sustained release of loaded proteins with a reduced initial burst.[20–23] Our recent study demonstrated that controlled BMP-2 delivery can be achieved by apatite coating and BMP-2-loaded scaffolds enhance osteogenesis of adipose-derived stem cells (ASCs) *in vitro* and promote bone regeneration in rodent models.[24] Although previous studies have demonstrated that phenamil can induce osteogenic differentiation by enhancing BMP activity, and combined application of phenamil with BMP-2 can enhance osteogenesis *in vitro*,[14,16–19] no single study reported the ability of phenamil to promote bone regeneration and how phenamil delivery influences BMP-2-mediated bone formation *in vivo*.

This study investigates whether phenamil can maximize BMP-2-induced bone formation and lower the BMP-2 dose requirement without compromising osteogenic efficacy. The ability of phenamil to promote osteogenic differentiation of ASCs was observed with the addition of different concentrations of BMP-2 *in vitro*. We further evaluated the complementary strategy of phenamil + BMP-2 to enhance bone regeneration in a calvarial defect model by using apatite-coated PLGA (Ap-PLGA) scaffolds fabricated to slowly release phenamil and BMP-2. We first determined the optimal therapeutic phenamil dose providing the most robust bone formation. In this dose range, we tested whether phenamil can enhance BMP-2-mediated bone formation and potentially reduce the BMP-2 dose without compromising osteogenic efficacy.

Materials and Methods

Materials

PLGA was purchased from Durect Corp (Pelham, AL). Collagenase I, 5-Brom-4-chlor-3-indoxylphosphat (BCIP), Nitro Blue tetrazolium (NBT), Alizarin Red, L-ascorbic acid, β-glycerophosphate, dexamethason, *p*-nitrophenol phosphate, and phenamil were purchased from Sigma-Aldrich (St. Louis, MO). BMP-2 and ELISA assay kit were purchased from R&D Systems (Minneapolis, MN). NP-40 cell lysis buffer, Live/Dead assay, PicoGreen dsDNA Assay, TRIzol, and cDNA transcription kit were purchased from Life Technologies (Grand Island, NY). C57/BL mouse and nude mouse were purchased from Charles River Laboratories (Wilmington, MA). Polyclonal antibody (Trb3, Smurf1, Smad1/5/8, and GAPDH), and Trb3-targeted siRNA were purchased from Santa Cruz Biotechnology (Santa Cruz, CA). RNeasy Mini Plant kit was purchased from Qiagen (Valencia, CA).

Cell isolation and culture

ASCs were isolated from inguinal fat pads of C57BL/6 mouse (4–8 weeks) as previously described.[23] Adipose tissues were harvested, rinsed in sterilized phosphate-buffered saline (PBS), cut into small pieces, and digested with 0.1% collagenase type I. After 2 h of digestion in incubators, cells were released from adipose tissues, collected by centrifugation at 1200 rpm for 5 min, and then resuspended in growth medium including low glucose Dulbecco's Modified Eagle's Medium (LDMEM), 10% fetal bovine serum (FBS), and 1% penicillin/streptomycin (100 U/mL) (P/S). The resuspended cells were seeded onto the tissue culture flasks. The ASCs at passage 4 were utilized for further experiments.

Alkaline phosphatase activity and Alizarin red staining

ASCs were cultured in growth medium. When cells arrived at almost 100% confluence, the growth medium was changed to an osteogenic medium containing 10 mM β-glycerophosphate, 50 μg/mL L-ascorbic acid, and 100 nM dexamethasone and the culture medium was supplemented with various concentrations of BMP-2 (0, 25, 50, or 100 ng/mL) in the presence or absence of phenamil (20 μM). After 3 days of culture, alkaline phosphatase (ALP) staining was performed as previously described.[23] Briefly, cells were fixed in 10% formalin for 15 min, washed with PBS, and incubated in a solution consisting of NBT and BCIP stock solutions in AP buffer (100 mM Tris pH 8.5, 50 mM $MgCl_2$, and 100 mM NaCl) for 1 h. The stained samples were observed with the Olympus BX51 microscope. ALP expression was detected in blue. For the colorimetric measurement of ALP activity, cells were washed with PBS and solubilized in lysis buffer (0.2% NP-40, 1 mM magnesium chloride) at 4°C for 30 min. ALP activity was determined using *p*-nitrophenol phosphate as a substrate and measuring at an absorbance at 405 nm. Measurements were performed in triplicate and normalized to total DNA content determined by the PicoGreen dsDNA Assay.

Alizarin red staining was performed as previously described.[23] After 14 days of culture, cells were fixed in 10% formalin for 15 min, washed with PBS, and incubated in 2% Alizarin red staining solution for 5 min. The stained samples were then observed with the Olympus BX51 microscope. Calcium deposition was detected in red. The quantification of mineralization was performed as previously described.[25] Briefly, the stained cells were dissolved in 10% (v/v) acetic acid and Alizarin red absorbance was assayed at 405 nm.

RNA extraction and quantitative real-time polymerase chain reaction

Total RNA was extracted using TRIzol reagent and RNeasy Mini Plant kit as previously described.[23] Briefly, 0.5 μg of total RNA was reversely transcribed to cDNA using a cDNA transcription kit. Quantitative real-time PCR was measured using LightCycler 480 PCR (Indianapolis, IN) with 20 μL SYBR Green reaction system. PCR amplification was performed for 45 cycles. The expression of *GAPDH* was utilized to normalize gene expression. The following primers were used in this experiment — *GAPDH*: AGGTCGGTGTGAACGGATTTG (forward), TGTAGAC

CATGTAGTTGAGGTCA (reverse); *Osterix*: GCTAGAGA TCTGAGCCGGGTA (forward); AAGAGAGCCTGGCAA GAGG (reverse); *Runx2*: CGGTCTCCTTCCAGGATGGT (forward), GCTTCCGTCAGCGTCAACA (reverse); *ALP*: GTTGCCAAGCTGGGAAGAACAC (forward), CCCACC CCGCTATTCCAAAC (reverse); *Osteocalcin (OCN)*: GGG AGACAACAGGGAGGAAAC (forward), CAGGCTTCCT GCCAGTACCT (reverse); *Osteopontin (OPN):* CTCCTGG CTGAATTCTGAGG (forward), TGCCAGAATCAGTCA CTTTCA (reverse); *Trb3*: CTGAGGCTCCAGGACAAGA (forward), CCTGCAGGAAACATCAGCA (reverse).

Western blot assay

Cells were lysed in NP-40 cell lysis buffer. Protein concentration was determined using bicinchoninic acid (BCA) protein assay (Thermo Scientific, Rockford, IL). The proteins were fractionated by SDS–polyacrylamide gel electrophoresis, transferred onto Immobilon polyvinyl difluoride (PVDF) membrane (Millipore, Billerica, MA) and immunoblotted by polyclonal antibody for Trb3, Smurf1, Smad1/5/8, and GAPDH, respectively. The membrane was then incubated with horseradish peroxidase (HRP)-conjugated secondary antibody (Millipore). The immunoreactive proteins were subsequently detected by Chemiluminescent HRP (Denville Scientific, Inc., South Plainfield, NJ).

Preparation of scaffolds

PLGA scaffolds were fabricated by the solvent casting and particulate leaching technique as previously described.[20] Briefly, PLGA/chloroform solutions were mixed with 200–300 μm diameter sucrose to obtain 92% porosity (volume fraction), and compressed into thin sheets in a Teflon mold. Scaffolds were dried in a fume hood and solvents were removed by freeze-drying at 100 mTorr and −110°C (SP Industries, Inc., Warminster, PA) overnight. Sucrose was removed by immersing scaffolds in double-distilled (dd) H_2O. Scaffolds were disinfected by immersion in 70% ethanol for 30 min, followed by three rinses of ddH_2O. Finally, the obtained scaffolds were cut into a diameter of 3 mm for further studies.

Biomimetic apatite coating process

Apatite coating solution was prepared as described in our prior studies.[20,22] Briefly, simulated body fluids (SBF) were prepared by sequentially dissolving $CaCl_2$, $MgCl_2 \cdot 6H_2O$, $NaHCO_3$, and $K_2HPO_4 \cdot 3H_2O$ into ddH_2O. The solution was adjusted to pH 6.0 and then Na_2SO_4, KCl, and NaCl were added. The final solution was adjusted to pH 6.5 (SBF1). Mg^{2+} and HCO_3^- free SBF (SBF 2) was prepared by subsequently dissolving $CaCl_2$ and $K_2HPO_4 \cdot 3H_2O$ into ddH_2O and pH was adjusted to pH 6.0. KCl and NaCl were added and the solution was adjusted to pH 6.8. All solutions were sterile filtered through a 0.22 μm polyethersulfone membrane (Nalgene, Rochester, NY).The obtained scaffolds were subjected to glow discharge argon plasma etching (Harrick Scientific, Ossining, NY). The etched scaffolds were incubated in SBF 1 for 24 h and then changed to SBF 2 for another 24 h at 37°C. The apatite-coated scaffolds were washed with ddH_2O to remove excess ions and lyophilized before further studies.

Scanning electron microscopy

The internal morphology of Ap-PLGA scaffold was examined by scanning electron microscopy (SEM; Nova Nano SEM 230/FEI, Hillsboro, OR). The cross-sectioned samples were mounted on aluminum stubs and sputter-coated with gold at 20 mA under 70 mTorr for 50 s.

In vitro *release of BMP-2 and phenamil*

The release kinetics of BMP-2 and phenamil from Ap-PLGA was determined using ELISA and UV spectrometry, respectively. Briefly, BMP-2 and phenamil in PBS were dropped onto scaffolds at a final concentration of 10 μg/mL and 200 μM for BMP-2 and phenamil, respectively. The scaffolds were dried for 15 min under laminar flow and further lyophilized in a freeze dryer for 3 h. The loaded scaffolds were incubated in 1 mL of 10 mM PBS (pH 7.4) containing 10% FBS at 37°C. The whole incubating solution was removed and replaced with 1 mL fresh solution at predetermined time points over a span of 21 days. The amount of released BMP-2 in the supernatant was assayed using Elisa assay according to the manufacturer's protocol. The amount of released phenamil was measured by UV spectrometry at an absorbance at 366 nm. The experiment was performed in triplicate, and the amount of release was expressed as a percentage of the initial amount of loaded BMP-2 and phenamil.

Cell proliferation and differentiation on scaffolds

ASCs at passage 5 were seeded to Ap-PLGA scaffolds at a concentration of 3×10^6 cells/mL and cultured up to 14 days. To observe proliferation of the cells cultured on the scaffolds, the cell/scaffold constructs were stained with a Live/Dead staining kit at 37°C for 15 min and observed under a fluorescence microscope (Olympus, Lake Success, NY) at day 1, 7, and 14. Proliferation of cells on the scaffolds was further quantified with the alamarBlue assay kit. The cell/scaffold constructs were collected, washed with PBS, and incubated with sterilized alamarBlue solution for 3 h at 37°C. AlamarBlue fluorescence was assayed at 535 nm (excitation) and 600 nm (emission) in a plate reader.

For ALP activity, the cell/scaffold constructs were rinsed with PBS and homogenized in lysis buffer as described above. ALP activity was determined using *p*-nitrophenol phosphate at an absorbance at 405 nm and normalized to total DNA content. The experiments were performed in triplicate.

Calvarial defect model

The surgical procedures were performed in accordance with the guidelines of the Chancellor's Animal Research Committee at the University of California, Los Angeles. Calvaria of male 2-month-old CD-1 nude mice were exposed to a trephine drill under constant irrigation and 3-mm full-thickness craniotomy defects were created in each parietal bone with care to avoid injury to the underlying dura mater as previously described.[26] Each defect was syringed with sterile saline solution to remove bone debris and then implanted with scaffolds containing phenamil or/and BMP-2 ($n = 8–12$). Phenamil was applied to Ap-PLGA scaffolds at final concentrations of 100, 300, 600, 1000, and 1500 μM as

described above. BMP was applied to scaffolds at final concentrations of 30, 60, and 100 μg/mL. Blank scaffolds were regarded as a control group. After surgery, all animals were allowed to recover on a warm sheet and then transferred to the vivarium for postoperative care. To get operative treatment, all animals received analgesia with subcutaneous injections of buprenorphine with a concentration of 0.1 mg/kg for up to 3 days. To prevent potential infection, all animals also received drinking water including trimethoprim-sulfamethoxazole for up to 7 days.

Three-dimensional micro-computerized tomography scanning

After 6 weeks postimplantation, animals were sacrificed and calvarial tissues were harvested for analysis. The extracted calvarial tissues were fixed in 4% formaldehyde at room temperature with gentle shaking. After 48 h, the fixed samples were rinsed with PBS and stored in 70% ethanol at 4°C before imaging using the high-resolution microCT machine (μCT SkyScan 1172; SkyScan, Kontich, Belgium) utilizing 57 kVp, 184 μA, 0.5 mm aluminum filtration, and 10 μm resolution. Visualization and reconstruction of the data were obtained by using Dolphin 3D software (Dolphin Imaging & Management Solutions, Chatsworth, CA). New bone volume was analyzed using CTAn software (Skyscan, Kontich, Belgium) and new bone area was analyzed using Image J software (NIH, Bethesda, Maryland). Bone-specific analysis included new bone area/original defect size (% area) and new bone volume/tissue volume (% volume).

Histological evaluation

The fixed tissues were decalcified under 10% ethylenediaminetetraacetic acid (EDTA) solution under gentle shaking for 1 week. The EDTA solution was replaced once at day 3. Decalcified samples were embedded in paraffin and cut into sections of 5 μm thickness. The tissue sections were deparaffinized and stained with hematoxylin and eosin (H&E). Masson's trichrome staining was also performed to detect new bone formation. The light green solution was used to stain bone tissue. The green color indicated new or mature bone, observed using a microscope.

Statistical analysis

Statistical analysis was performed using one-way analysis of variances (ANOVA), with the Tukey's *post hoc* test when more than two groups were compared. A Student's *t-t*est was used to directly compare two groups. p value less than 0.05 was considered statistically significant.

Results

Osteogenesis of ASCs by phenamil and BMP-2

Treatment of ASCs with phenamil significantly induced osteogenic differentiation in a dose-dependent manner up to 20 μM (Supplementary Fig. S1; Supplementary Data are available online at www.liebertpub.com/tea). Using this dose range, we investigated whether phenamil can enhance BMP-2 induced osteogenesis of ASCs.

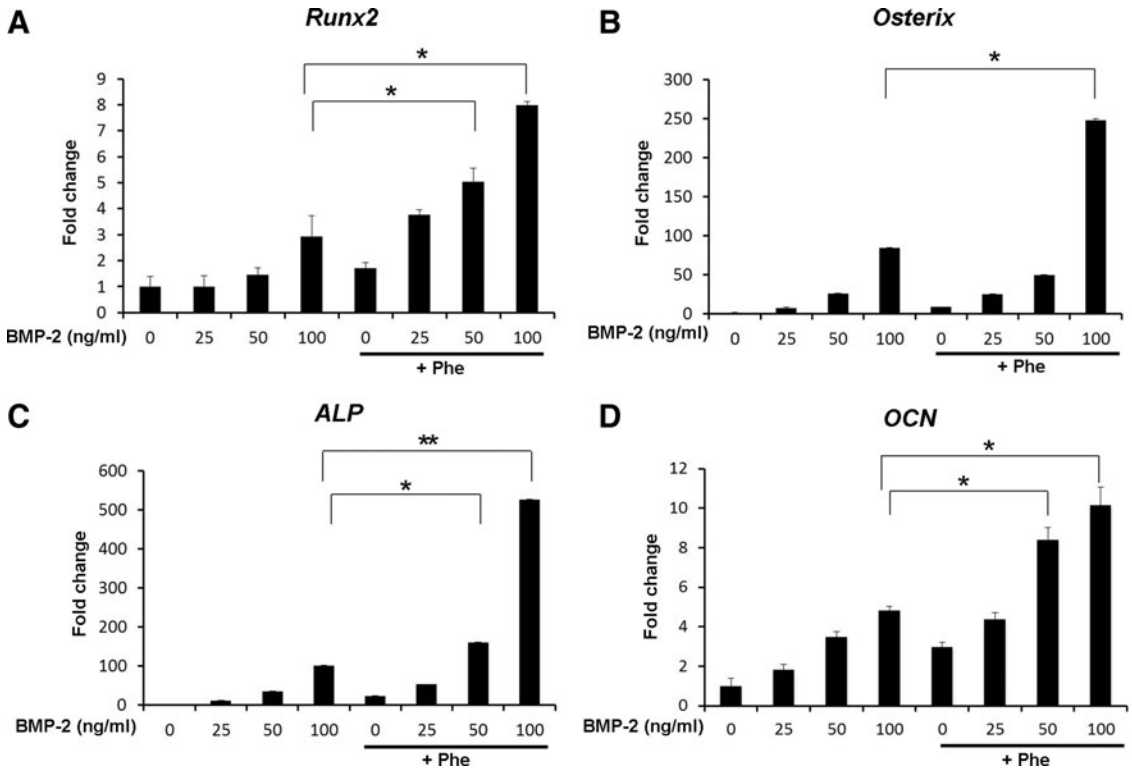

FIG. 1. Expression of *Runx2* **(A)**, *Osterix* **(B)**, *ALP* **(C)**, and *OCN* **(D)** in adipose-derived stem cells (ASCs) treated with phenamil and bone morphogenetic protein (BMP)-2 at day 3. Expression of the osteogenic gene markers upregulated by BMP-2 was significantly enhanced in the presence of phenamil (*$p < 0.05$, **$p < 0.01$).

Osteogenic markers were confirmed by gene expression analysis using quantitative real-time polymerase chain reaction (qRT-PCR) in ASCs cultured with various concentrations of BMP-2 in combination with 20 μM phenamil for 3 days (Fig. 1). Expression of *ALP*, an early osteogenic marker, was increased 10.7- to 100.4-fold as the BMP concentration increased from 25 to 100 ng/mL. Addition of phenamil (20 μM) significantly increased BMP-2-induced *ALP* expression 52.6- to 526.4-fold (Fig. 1C). The expression level of *ALP* in ASCs treated with 25 ng/mL BMP-2 and phenamil was comparable to that detected in ASCs stimulated with 100 ng/mL BMP-2 alone (Fig. 1C). *Runx2* and *Osterix* are critical regulators in osteogenic differentiation. When stimulated with 100 ng/mL BMP-2 and 20 μM phenamil, the expression of *Runx2* and *Osterix* increased 2.9- to 8- fold and 84.3- to 247.8-fold, respectively, compared with control cells (Fig. 1A, B). Given the high ability of phenamil + BMP-2 stimulation to accelerate osteogenesis, we monitored expression of *OCN*, a late osteogenic marker, gene as early as day 3. Co-treatment of ASCs with phenamil and BMP-2 significantly increased the expression of *OCN* compared with cells treated with phenamil or BMP-2 alone (Fig. 1D).

To further confirm early osteogenic differentiation observed in the mRNA expression levels of *ALP*, we assessed

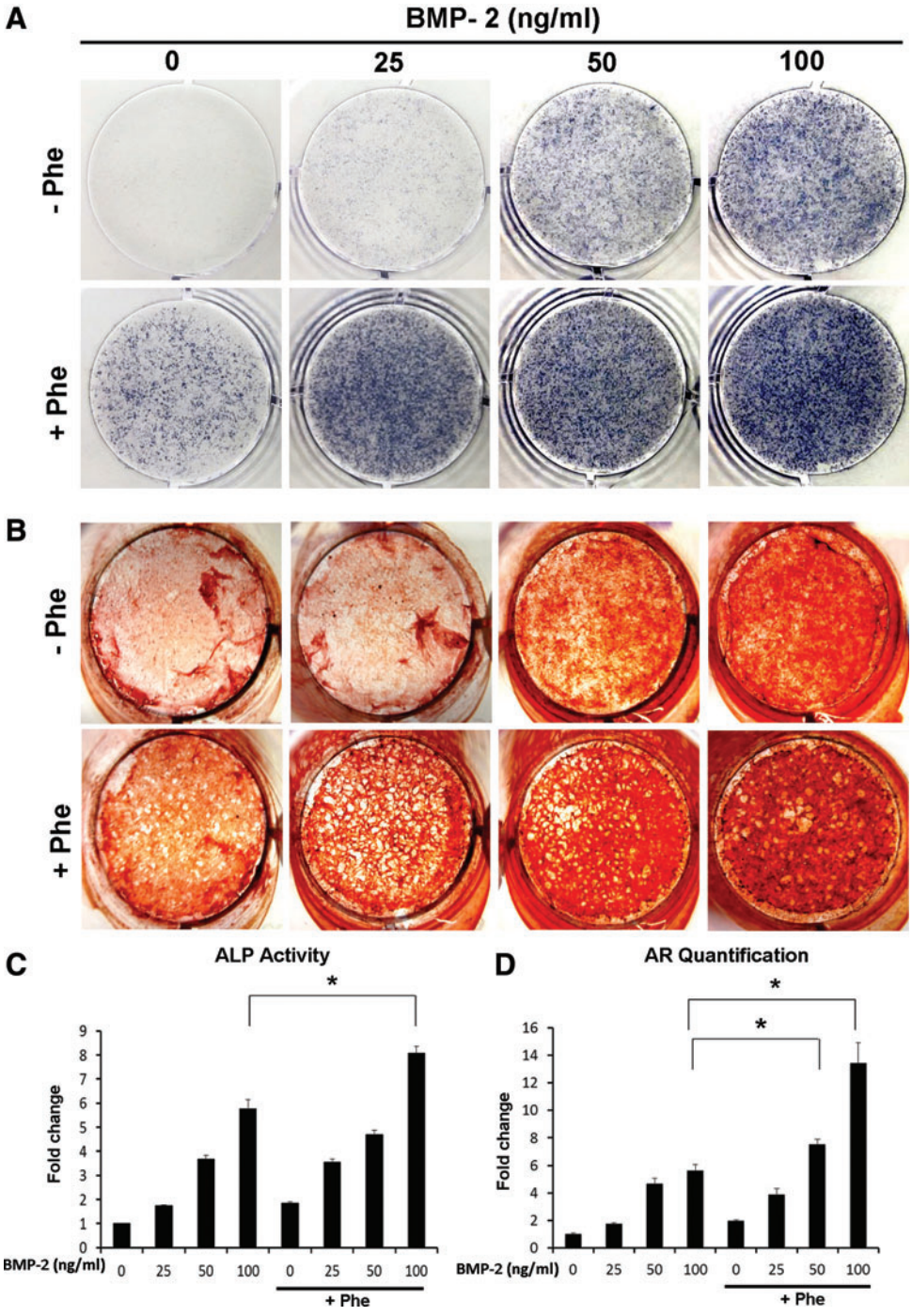

FIG. 2. Phenamil enhanced BMP-2-induced osteogenic differentiation of ASCs. **(A)** Alkaline phosphatase (ALP) staining at day 3. **(B)** Alizarin red (AR) staining at day 21. **(C)** ALP activity at day 3 (*$p < 0.05$). **(D)** Quantification of Alizarin red staining at day 21. *$p < 0.05$. Color images available online at www.liebertpub.com/tea

ALP activity by detecting ALP production through histochemical and colorimetric assays (Fig. 2A, C). ALP activity was increased 1.8- to 5.8-fold as the BMP concentration increased from 25 to 100 ng/mL (Fig. 2C) after 3 days of culture. Addition of phenamil (20 μM) further increased ALP activity 8.1-fold with 100 ng/mL BMP-2 treatment, which was significantly higher than that detected in ASCs treated with phenamil or BMP-2 alone (Fig. 2C).

Mineralization was further evaluated by Alizarin Red staining at day 21 (Fig. 2B). BMP-2 treatment (from 25 to 100 ng/mL) dose dependently enhanced mineralization in ASCs 1.7- to 5.6-fold, which was further increased 3.9- to 13.4-fold with phenamil treatment (20 μM) compared with ASCs treated with BMP-2 alone (Fig. 2D). Stimulation of ASCs with 20 μM phenamil + 25 ng/mL BMP-2 resulted in mineralization comparable to that detected in ASCs stimulated with 50 ng/mL BMP-2 (Fig. 2D). Mineralization of ASCs treated with 20 μM phenamil + 50 ng/mL BMP-2 was significantly higher than that detected in ASCs stimulated with 100 ng/mL BMP-2.

Trb3 in phenamil-mediated osteogenesis

Phenamil has been shown to induce BMP signaling and osteogenic differentiation through upregulation of Trb3.[14] Phenamil increased the expression of *Trb3* gene in ASCs in the presence or absence of BMP-2 (100 ng/mL), consistent with previous findings (Supplementary Fig. S2). To evaluate effect of phenamil treatment on BMP signaling in ASCs, we have performed western blot for Trb3, Smurf1, and Smads (Smad1/5/8) (Fig. 3). Trb3 protein expression was increased with phenamil stimulation for 3 days in the presence or absence of BMP-2. Increased Trb3 downregulated Smurf1 and enhanced levels of Smads, major signal transducers for BMP-2.

To further investigate the role of Trb3 in phenamil-induced osteogenesis, Trb3 suppression in ASCs was induced using Trb3-targeting siRNA. Expression of Trb3 protein was greatly decreased with Trb3 siRNA transduction at 3 days after treatment with or without phenamil as validated by western blot (Fig. 4A). Knockdown of Trb3 significantly reduced phenamil-induced osteogenic differentiation of ASCs indicated by ALP staining at day 3 (Fig. 4B). qRT-PCR analysis demonstrated that Trb3 siRNA treatment did not alter the expression of *Osterix* and *OPN* compared with control siRNA-treated ASCs in the presence or absence of BMP-2 at day 3, although the expression of *Trb3* was decreased in cells (Fig. 4C). In contrast, the results showed a significant decrease in the expression of *Osterix* and *OPN* induced by phenamil in the presence or absence of BMP-2 after Trb3 knockdown (Fig. 4C). These results suggested that phenamil induces ostogenic differentiation via mediator of Trb3 that can positively regulate BMP pathway.

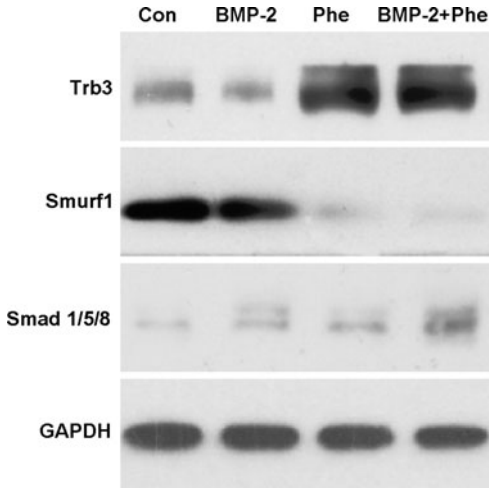

FIG. 3. Phenamil reduced Smurf1 and increased Smad1/5/8 levels by increasing Trb3. ASCs were treated with BMP-2 (100 ng/mL) or/and phenamil (20 μM) for 3 days and cell lysates were assayed by western blot analysis.

Release of phenamil and BMP-2 from scaffolds

To determine whether Ap-PLGA scaffolds can sustain the release of phenamil and BMP-2, PLGA was fabricated into 3D porous scaffolds, which were further modified with apatite coatings as described in our previous studies. A uniform layer of apatite coating was formed on the surface and the created coating resulted in plate-like morphology (Fig. 5A, B). Ap-PLGA scaffolds were loaded with 200 μM phenamil (282 ng per scaffold) and 10 μg/mL BMP-2 (100 ng per scaffold) and release kinetics were determined by incubating the scaffolds in serum solutions (PBS supplemented with 10% FBS). Our study showed that loaded phenamil was slowly released in a sustainable manner with approximately 28% of initial burst from scaffolds (Fig. 5C). ELISA assay showed that approximately 7% of initially loaded BMP-2 was released at day 1, followed by slow release up to day 21 (Fig. 5D).

ASC culture on scaffolds releasing phenamil and BMP-2

To evaluate the feasibility of Ap-PLGA scaffolds to support cell growth, ASCs were seeded on the scaffolds loaded with phenamil and/or BMP-2 and observed by Live/Dead staining (Fig. 6A). Our results showed a high level of viability (>95%) of seeded cells over the 21-day culture period in all scaffolds. The cells proliferated on the scaffolds over the culture period, as indicated by alamarBlue assay, and the scaffolds loaded with phenamil and/or BMP-2 significantly increased cell proliferation compared with control scaffolds (Fig. 6B). The bioactivity of phenamil or BMP-2 loaded on the scaffolds was assessed by observing ALP expression in ASCs seeded on the scaffolds (Fig. 6C). ASCs seeded on scaffolds releasing phenamil or BMP-2 significantly increased the expression level of ALP compared with that detected in control scaffolds. The expression of ALP was further enhanced in ASCs cultured on the scaffolds loaded with both phenamil and BMP-2, as compared to the scaffolds loaded with phenamil or BMP-2 alone.

Calvarial bone formation by phenamil

To analyze the ability of phenamil to induce bone regeneration, 3 mm critical-sized mouse calvarial defects were created and Ap-PLGA scaffolds loaded with various concentrations of phenamil were implanted (Supplementary Fig. S3). MicroCT imaging demonstrated increased bone regeneration in phenamil-treated defects with maximum bone

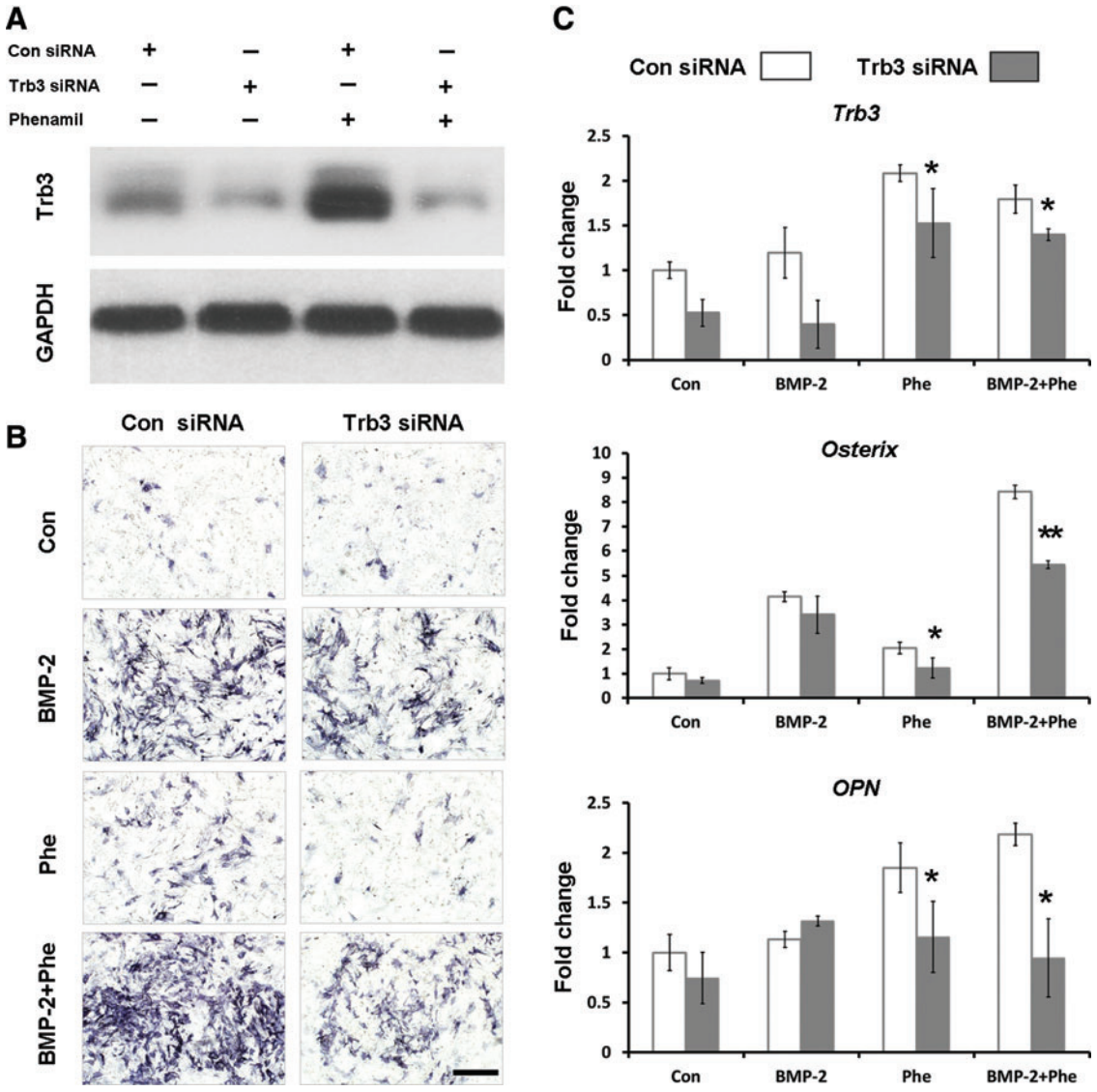

FIG. 4. Phenamil induced osteogenic differentiation of ASCs through Trb3 expression. **(A)** Western blot analysis of Trb3 levels in ASCs transduced with Trb3-targeting siRNA in the presence or absence of phenamil (20 μM) at day 3. **(B)** ALP Expression in ASCs transduced with Trb3-targeting siRNA in the presence of BMP-2 (100 ng/mL) or/and phenamil (20 μM) at day 3. Scale bar = 500 μm **(C)** Gene expression of *Trb3* and osteogenic gene markers (*Osterix* and *OPN*) in ASCs at day 3. Trb3 knockdown significantly reduced phenamil-induced osteogenic gene expression in the presence or absence of BMP-2 ($*p < 0.05$, $**p < 0.01$). Color images available online at www.liebertpub.com/tea

formation at around 300–600 μM compared with control defects implanted with blank scaffolds at 6 weeks (Fig. 7A).

Quantitative analysis of microCT images was performed by observing new bone area and volume within the defects (Fig. 7B, C). Results revealed that defects treated with scaffold only showed percentage healing of approximately 18% and 6.3% by new bone area and bone volume, respectively, after 6 weeks. In contrast, defects treated with phenamil showed a significant increase in healing percent after 6 weeks, amounting to 77% of bone area and 37% of bone volume, as the phenamil dose increased up to 300 μM. Further increase of the phenamil dose beyond 300 μM decreased the percent area and volume healed.

The new bone formation was further characterized by histological examination (Fig. 8). H&E staining showed that defects treated with scaffold only were filled with soft tissue and minimal bone formation was observed at 6 weeks (Fig. 8A). New bone formation was apparent in defects treated with phenamil, which was superior with 300 μM phenamil treatment compared with other groups. Masson's trichrome staining revealed formation of osteoid matrix in defects treated with 100–600 μM phenamil, while control groups exhibited fibrous-like tissue with minimal bone formation (Fig. 8B).

Calvarial bone formation by phenamil and BMP-2

We further evaluated combined effects of phenamil + BMP-2 on calvarial defect healing using scaffolds loaded with phenamil and BMP-2 (Fig. 9). Since 300 μM phenamil

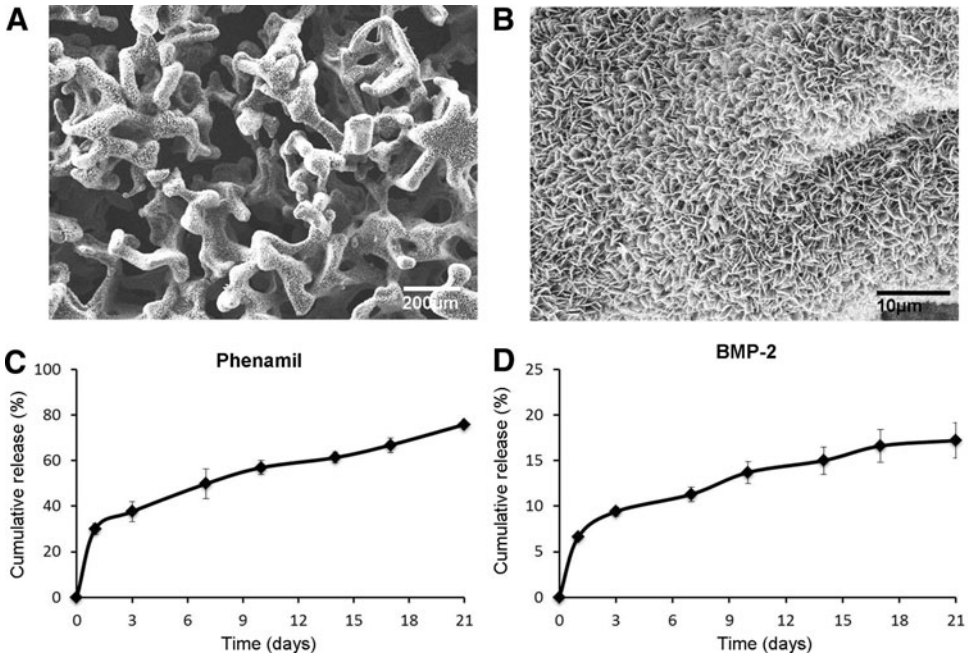

FIG. 5. SEM images of apatite-coated PLGA scaffolds (Ap-PLGA) at low **(A)** and high **(B)** magnification. *In vitro* release of phenamil **(C)** and BMP-2 **(D)** from apatite-coated PLGA scaffolds. SEM, scanning electron microscopy.

dose showed the most robust calvarial healing, the same final concentration of 300 μM was tested in combination with various concentrations of BMP-2 (30, 60, or 100 μg/mL). MicroCT demonstrated the addition of 300 μM phenamil to BMP-2 treated defects significantly increased bone regeneration compared with defects treated with BMP-2 alone (Fig. 9A).

Quantitative analysis revealed that the amount of bone formation in defects treated with 300 μM phenamil + 30 μg/mL BMP-2 (96% of bone area and 55.1% of bone volume)

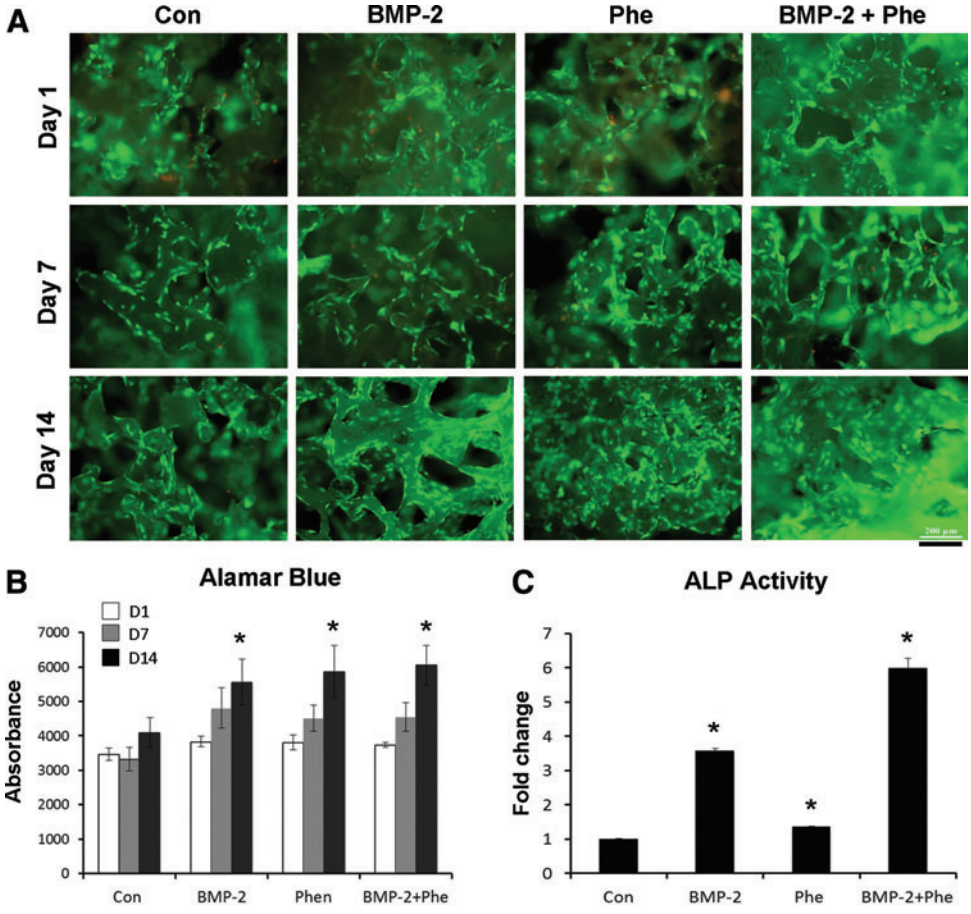

FIG. 6. Growth of ASCs in the apatite-coated PLGA scaffolds loaded with BMP-2 or/and phenamil. **(A)** Live-dead fluorescent staining at day 1, 7, and 14. Scale bar = 200 μm **(B)** AlamarBlue assay showing cell proliferation (*$p < 0.05$ compared with control). **(C)** ALP activity showing bioactivity of BMP-2 and phenamil loaded on scaffolds (*$p < 0.05$ compared with control). Color images available online at www.liebertpub.com/tea

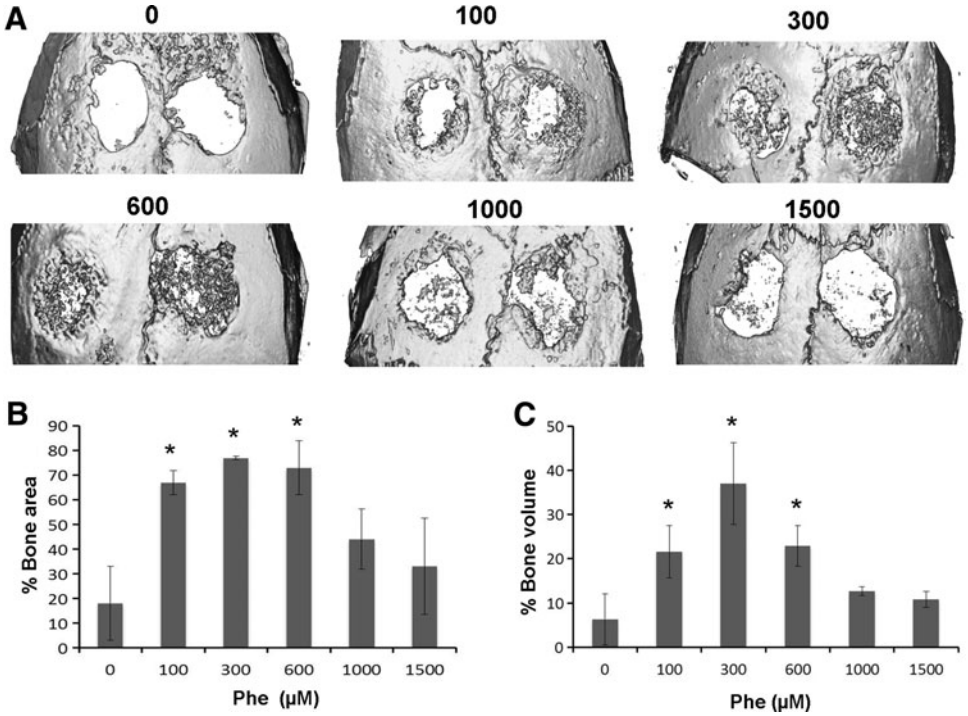

FIG. 7. **(A)** Micro-computed tomography images of calvarial defects treated with Ap-PLGA scaffolds loaded with various doses of phenamil (0, 100, 300, 600, 1000, and 1500 μM). Quantification of percentage area **(B)** and volume **(C)** bone regeneration in calvarial defects. *Significant higher bone formation compared with control ($*p < 0.05$).

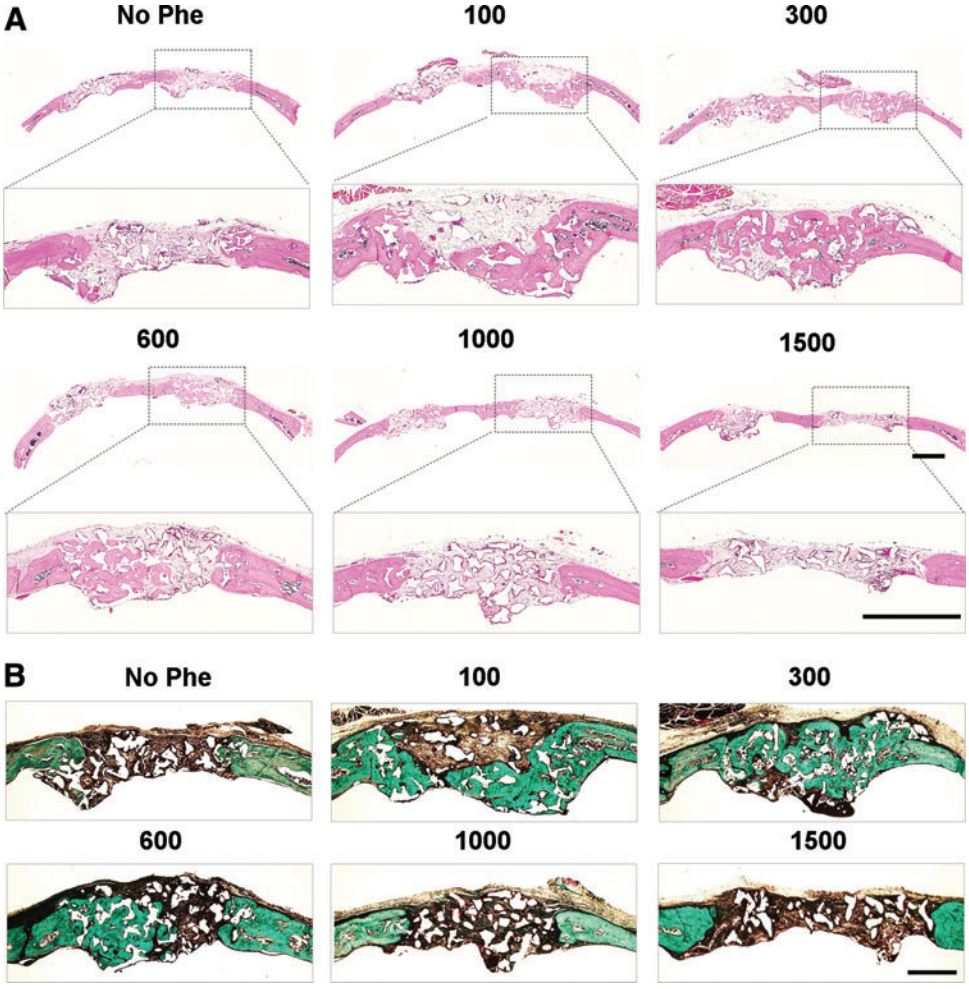

FIG. 8. Histological analysis of bone regeneration in calvarial defects treated with various doses of phenamil (0, 100, 300, 600, 1000, and 1500 μM). **(A)** Hematoxylin-eosin staining. Scale bar = 1 mm. **(B)** Masson's trichrome staining. Scale bar = 500 μm. Color images available online at www.liebertpub.com/tea

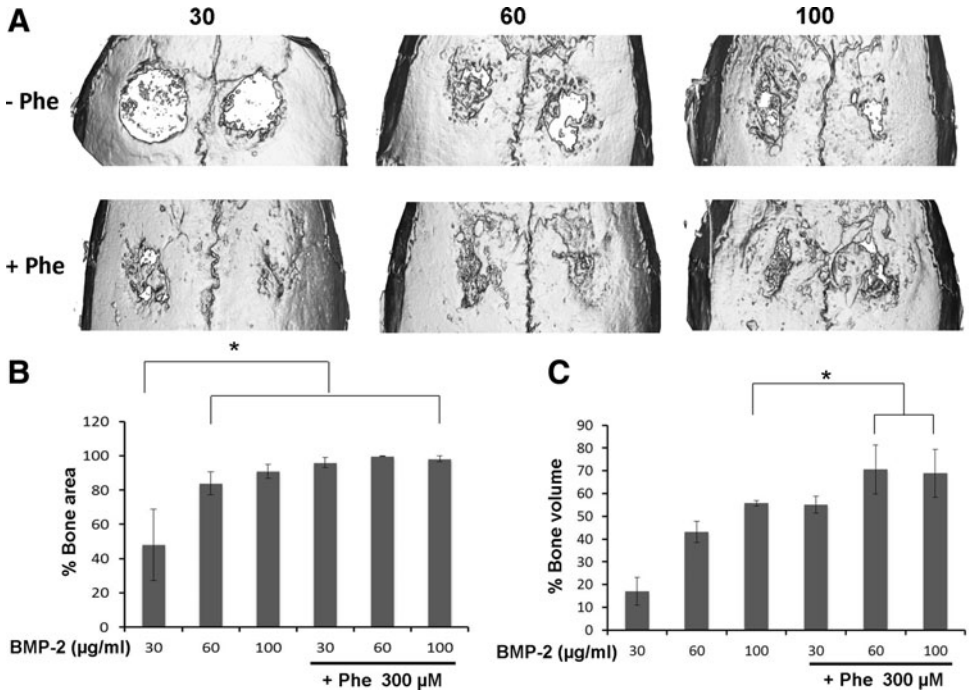

FIG. 9. **(A)** Micro-computed tomography images of calvarial defects treated with Ap-PLGA scaffolds loaded with various doses of BMP-2 (30, 60, and 100 μg/mL) in the presence or absence of phenamil (300 μM). Quantification of percentage area **(B)** and volume **(C)** bone regeneration in calvarial defects ($*p < 0.05$).

was comparable to that of defects treated with three-fold more BMP-2 (100 μg/mL) alone (91% of bone area and 55.7% of bone volume) (Fig. 9B, C). Although the further increase of BMP-2 up from 30 to 100 μg/mL did not alter new bone area in defects treated with phenamil and BMP-2, the co-treatment significantly increased bone volume healed.

MicroCT findings were further confirmed by H&E staining (Fig. 10A) and Masson's trichrome staining (Fig. 10B). Histological analysis revealed that phenamil + BMP-2 groups had more mature bone formation completely bridging the defect area, while no obvious bone bridge formation was found in defects treated with BMP-2 alone. Moreover, infiltration of bone marrow was apparent under new bone bridge in co-treated defects, in contrast to defects treated with BMP-2 alone.

Discussion

A number of osteoinductive factors have been studied in an attempt to enhance bone regeneration and eliminate complications associated with bone graft harvest.[4,27] Among the various osteoinductive factors available, BMPs have received solid attention for exerting strong effects on osteogenic differentiation of progenitor cells and are currently approved for spinal fusion, fracture healing, and maxillofacial regeneration.[28] While BMPs have successfully induced bone formation *in vivo*, high dose requirements and paradoxical activities of BMPs on progenitor cells may lead to unexpected side effects such as ectopic bone formation while also rendering high treatment costs to patients.[5–8]

In this study, we employed a small molecule that can effectively complement the pro-osteogenic activity of BMP-2 to maximize biological efficiency, thereby reducing the total dose requirement (cost) and minimizing potential adverse effects associated with BMP-2. Small molecular therapeutics has several advantages over protein-based therapeutics due to their lower cost and ease of manufacturing and storage compared with growth factor proteins.[9] Moreover, small molecules readily penetrate cell membranes with their rapid and reversible biological activity, which make them attractive in cell-based therapies and regenerative medicine.[9]

Phenamil is a derivative of the FDA-approved diuretic amiloride, an inhibitor of ion transporters.[14,19] A previous study reported that phenamil induced osteoblastic differentiation and mineralization in bone marrow-derived mesenchymal stem cells (MSCs).[14] MSCs isolated from adipose tissue are considered excellent candidates in cell-based bone tissue engineering strategies due to their ease of harvesting and abundant stem cell pool in the tissue, and their high proliferative and differentiation properties into multiple lineages.[29,30] This study demonstrated that treatment of ASCs with phenamil significantly enhanced osteogenic differentiation of cells as shown by upregulation of osteogenic gene expression and mineral formation. Phenamil-induced osteogenic differentiation of ASCs was significantly higher in combination with BMP-2 treatment than that detected in ASCs treated with phenamil or BMP-2 alone.

The observed enhanced osteogenesis by the combination of phenamil and BMP-2 can be explained by phenamil stimulation of BMP-2 responsiveness through increasing the expression of Trb3 protein and subsequently promoting the production of Smad signaling, major signal transducers for BMP-2. It has been demonstrated that increased Trb3 triggered degradation of SMAD ubiquitin regulatory factor 1 (Smurf1), a negative regulator of Smads, thereby potentiating BMP signaling.[14,15,31] In this study, western blot analysis showed that phenamil reduced Smurf1 protein levels and increased Smad1/5/8 levels by inducing Trb3 expression. Moreover, the combined treatment of BMP-2 + Phenamil resulted in greater upregulation of Smads than the addition of either factor alone, as shown in these data. In contrast, knockdown of Trb3 significantly reduced phenamil-induced

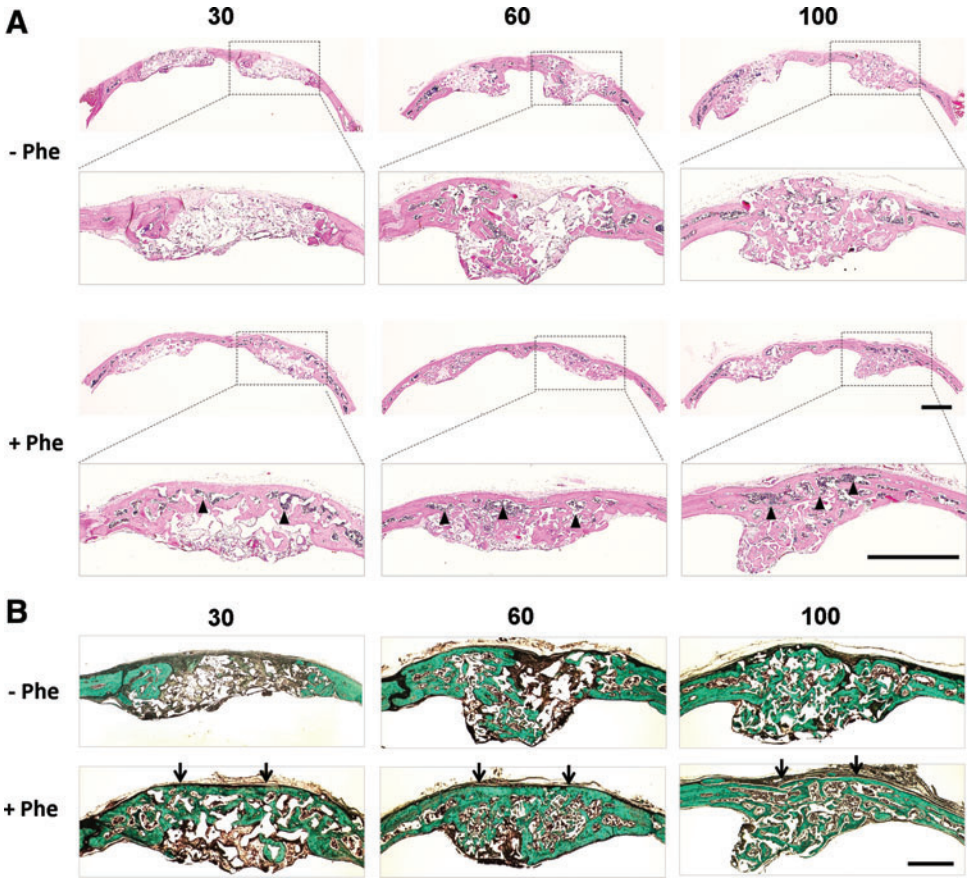

FIG. 10. Histological analysis of bone regeneration in calvarial defects treated with various doses of BMP-2 (30, 60, and 100 μg/mL) in the presence (+Phe) or absence (−Phe) of phenamil (300 μM). **(A)** Hematoxylin-eosin staining. Scale bar = 1 mm. **(B)** Masson's trichrome staining. Scale bar = 500 μm. Bone bridge formation (*arrows*) with infiltration of bone marrow (*arrowheads*) was obvious in defects treated with phenamil + BMP-2. Color images available online at www.liebertpub.com/tea

osteogenic differentiation of ASCs in the presence or absence of BMP-2, confirming previous results that Trb3 may be a critical mediator in BMP signaling and osteogenic differentiation. Taken together, our data suggested that phenamil can work additively or synergistically with BMP-2 to maximize activity of the BMP pathway in bone regeneration.

Therapeutic efficacy of osteoinductive molecules is dose related and affected by delivery kinetics due to their intrinsic instability and fast degradation requiring large concentrations for their therapeutic uses. Thus, it is necessary to develop appropriate carriers capable of delivering biological molecules over time in a controlled manner in a target tissue defect. In this study, we utilized Ap-PLGA scaffolds to deliver BMP-2 and phenamil. We previously developed a biomimetic process to create apatite layers on various biomaterial surfaces, and the created apatite provided a favorable substrate for cell adhesion and osteogenic differentiation.[20,22–24] This study showed that loaded BMP-2 and phenamil were slowly released in a sustainable manner with approximately 7% and 29% of initial burst from scaffolds, respectively. The observed sustained release of BMP-2 can be attributed to increased electrostatic interaction between BMP-2 and charged binding sites on the apatite surface. Moreover, the created apatite exhibited plate-like morphology with increased surface area that may play a role in reducing initial burst of BMP-2 and phenamil by increasing drug retention capacity. Similar sustained release of BMP-2 was observed on the apatite coating created on CH scaffolds in our previous study.[24] It was also demonstrated that calcium phosphate substrates supported controlled delivery of bisphosphonate or simvastatin molecules.[32–34] Other studies indicated that release of adsorbed molecules can be affected by the chemical and structural characteristics (e.g., Ca/P ratio, crystallinity, surface texture) of the calcium phosphate substrates.[35–37]

We further investigated the ability of phenamil to induce bone regeneration in calvarial defect model well established in our previous studies. The microCT and histological analysis demonstrated phenamil induced significant bone formation with maximal calvarial healing at around 300 μM. The addition of 300 μM phenamil to BMP-2-treated defects significantly increased bone regeneration over defects treated with BMP-2 alone. Most interestingly, co-treatment of defects with phenamil and BMP-2 (30 μg/mL) induced equivalent level of bone formation as defects treated with threefold more BMP-2 (100 μg/mL) alone. These results suggest that phenamil can significantly reduce the clinical BMP-2 doses required for effective therapeutic results without compromising bone regeneration efficacy. However, phenamil had a narrow therapeutic window and its effective dose was close to the toxic dose. Further increasing the phenamil dose above 300 μM did lead to a significant decrease in bone formation. The observed reduced bone formation may be due to poor water solubility of phenamil, resulting in low drug bioavailability at the defect site. In addition, there is a possibility of increased toxicity and reduced hydrophilic nature of a scaffold surface with high phenamil loading that often prevents preferential cell recruitment and new bone formation. Additional study on delivery modalities of hydrophobic drugs in aqueous environments will be needed for effective and safer delivery of phenamil.

Although the osteogenic effect of phenamil and BMP-2 is species-specific and the results derived in a mouse model do not necessarily predict the most optimal phenamil + BMP-2 combination in humans, the results obtained from this study will establish novel complementary bone formation strategies using BMP-2 along with phenamil or related molecules.

Conclusions

In this study, we investigated a novel strategy to enhance bone regeneration using BMP-2 in combination with a small molecule that can effectively complement the osteogenic activity of BMP-2. We demonstrated that phenamil can additively work with BMP-2 to increase osteogenic differentiation ASCs. With a scaffold designed to release phenamil and BMP-2, we observed significantly enhanced bone regeneration in calvarial defects as compared with defects treated with BMP-2 alone. Results suggest that the combination strategy of phenamil and BMP-2 in bone repair may lead to more efficient and cost-effective therapeutic strategies.

Acknowledgments

This work was supported by the National Institutes of Health grants R01 AR060213 and R21 DE021819, the International Association for Dental Research, and the Academy of Osseointegration.

Disclosure Statement

No competing financial interests exist.

References

1. Kneser, U., Schaefer, D.J., Polykandriotis, E., and Horch, R.E. Tissue engineering of bone: the reconstructive surgeon's point of view. J Cell Mol Med **10,** 7, 2006.
2. Tatum, S.A., and Kellman, R.M. Cranial bone grafting in maxillofacial trauma and reconstruction. Facial Plast Surg **14,** 117, 1998.
3. Baqain, Z.H., Anabtawi, M., Karaky, A.A., and Malkawi, Z. Morbidity from anterior iliac crest bone harvesting for secondary alveolar bone grafting: an outcome assessment study. J Oral Maxillofac Surg **67,** 570, 2009.
4. Glassman, S.D., Carreon, L.Y., Djurasovic, M., Campbell, M.J., Puno, R.M., Johnson, J.R., and Dimar, J.R. RhBMP-2 versus iliac crest bone graft for lumbar spine fusion: a randomized, controlled trial in patients over sixty years of age. Spine (Phila Pa 1976) **33,** 2843, 2008.
5. Cahill, K.S., Chi, J.H., Day, A., and Claus, E.B. Prevalence, complications, and hospital charges associated with use of bone-morphogenetic proteins in spinal fusion procedures. JAMA **302,** 58, 2009.
6. Aghaloo, T., Jiang, X., Soo, C., Zhang, Z., Zhang, X., Hu, J., Pan, H., Hsu, T., Wu, B., Ting, K., and Zhang, X. A study of the role of nell-1 gene modified goat bone marrow stromal cells in promoting new bone formation. Mol Ther **15,** 1872, 2007.
7. Chen, N.F., Smith, Z.A., Stiner, E., Armin, S., Sheikh, H., and Khoo, L.T. Symptomatic ectopic bone formation after off-label use of recombinant human bone morphogenetic protein-2 in transforaminal lumbar interbody fusion. J Neurosurg Spine **12,** 40, 2010.
8. Perri, B., Cooper, M., Lauryssen, C., and Anand, N. Adverse swelling associated with use of rh-BMP-2 in anterior cervical discectomy and fusion: a case study. Spine J **7,** 235, 2007.
9. Laurencin, C.T., Ashe, K.M., Henry, N., Kan, H.M., and Lo, K.W. Delivery of small molecules for bone regenerative engineering: preclinical studies and potential clinical applications. Drug Discov Today **19,** 794, 2014.
10. Mundy, G., Garrett, R., Harris, S., Chan, J., Chen, D., Rossini, G., Boyce, B., Zhao, M., and Gutierrez, G. Stimulation of bone formation *in vitro* and in rodents by statins. Science **286,** 1946, 1999.
11. Zhou, Y., Ni, Y., Liu, Y., Zeng, B., Xu, Y., and Ge, W. The role of simvastatin in the osteogenesis of injectable tissue-engineered bone based on human adipose-derived stromal cells and platelet-rich plasma. Biomaterials **31,** 5325, 2010.
12. Dai, W., Dong, J., Fang, T., and Uemura, T. Stimulation of osteogenic activity in mesenchymal stem cells by FK506. J Biomed Mater Res A **86,** 235, 2008.
13. Isomoto, S., Hattori, K., Ohgushi, H., Nakajima, H., Tanaka, Y., and Takakura, Y. Rapamycin as an inhibitor of osteogenic differentiation in bone marrow-derived mesenchymal stem cells. J Orthop Sci **12,** 83, 2007.
14. Park, K.W., Waki, H., Kim, W.K., Davies, B.S., Young, S.G., Parhami, F., and Tontonoz, P. The small molecule phenamil induces osteoblast differentiation and mineralization. Mol Cell Biol **29,** 3905, 2009.
15. Chan, M.C., Nguyen, P.H., Davis, B.N., Ohoka, N., Hayashi, H., Du, K., Lagna, G., and Hata, A. A novel regulatory mechanism of the bone morphogenetic protein (BMP) signaling pathway involving the carboxyl-terminal tail domain of BMP type II receptor. Mol Cell Biol **27,** 5776, 2007.
16. James, A., Chung, C.G., Asatrian, G., Velasco, O., Halperin, D., Park, K.W., Bayani, G., Khadarian, K., Zhang, X., Ting, K., Tontonoz, P., and Soo, C. The Oral Small Molecule Phenamil Regulates BMP Signaling and Prevents Ovariectomy-Induced Osteoporosis. Abstract presented at the ASBMR Annual Meeting, Baltimore, MD, 2013. Abstract no. 1086.
17. Lo, K.W., Ulery, B.D., Kan, H.M., Ashe, K.M., and Laurencin, C.T. Evaluating the feasibility of utilizing the small molecule phenamil as a novel biofactor for bone regenerative engineering. J Tissue Eng Regen Med **8,** 728, 2014.
18. Kim, J.G., Son, K.M., Park, H.C., Zhu, T., Kwon, J.H., and Yang, H.C. Stimulating effects of quercetin and phenamil on differentiation of human dental pulp cells. Eur J Oral Sci **121,** 559, 2013.
19. Lo, K.W., Kan, H.M., and Laurencin, C.T. Short-term administration of small molecule phenamil induced a protracted osteogenic effect on osteoblast-like MC3T3-E1 cells. J Tissue Eng Regen Med 2013 [Epub ahead of print]; DOI: 10.1002/term.1786.
20. Chou, Y.F., Dunn, J.C., and Wu, B.M. *In vitro* response of MC3T3-E1 pre-osteoblasts within three-dimensional apatite-coated PLGA scaffolds. J Biomed Mater Res B Appl Biomater **75,** 81, 2005.
21. Hu, J., Hou, Y., Park, H., and Lee, M. Beta-tricalcium phosphate particles as a controlled release carrier of osteogenic proteins for bone tissue engineering. J Biomed Mater Res A **100,** 1680, 2012.
22. Park, H., Choi, B., Nguyen, J., Fan, J., Shafi, S., Klokkevold, P., and Lee, M. Anionic carbohydrate-containing

chitosan scaffolds for bone regeneration. Carbohydr Polym **97,** 587, 2013.
23. Fan, J., Park, H., Tan, S., and Lee, M. Enhanced osteogenesis of adipose derived stem cells with Noggin suppression and delivery of BMP-2. PLoS One **8,** e72474, 2013.
24. Fan, J., Park, H., Lee, M.K., Bezouglaia, O., Fartash, A., Kim, J., Aghaloo, T., and Lee, M. Adipose-Derived Stem Cells and BMP-2 Delivery in Chitosan-Based 3D Constructs to Enhance Bone Regeneration in a Rat Mandibular Defect Model. Tissue Eng Part A **20,** 2169, 2014.
25. James, A.W., Theologis, A.A., Brugmann, S.A., Xu, Y., Carre, A.L., Leucht, P., Hamilton, K., Korach, K.S., and Longaker, M.T. Estrogen/estrogen receptor alpha signaling in mouse posterofrontal cranial suture fusion. PLoS One **4,** e7120, 2009.
26. Aghaloo, T., Cowan, C.M., Chou, Y.F., Zhang, X., Lee, H., Miao, S., Hong, N., Kuroda, S., Wu, B., Ting, K., and Soo, C. Nell-1-induced bone regeneration in calvarial defects. Am J Pathol **169,** 903, 2006.
27. Epstein, N.E. Pros, cons, and costs of INFUSE in spinal surgery. Surg Neurol Int **2,** 10, 2011.
28. Valentin-Opran, A., Wozney, J., Csimma, C., Lilly, L., and Riedel, G.E. Clinical evaluation of recombinant human bone morphogenetic protein-2. Clin Orthop Relat Res **395,** 110, 2002.
29. Gimble, J.M., Katz, A.J., and Bunnell, B.A. Adipose-derived stem cells for regenerative medicine. Circ Res **100,** 1249, 2007.
30. Cowan, C.M., Shi, Y.Y., Aalami, O.O., Chou, Y.F., Mari, C., Thomas, R., Quarto, N., Contag, C.H., Wu, B., and Longaker, M.T. Adipose-derived adult stromal cells heal critical-size mouse calvarial defects. Nat Biotechnol **22,** 560, 2004.
31. Zhu, H., Kavsak, P., Abdollah, S., Wrana, J.L., and Thomsen, G.H. A SMAD ubiquitin ligase targets the BMP pathway and affects embryonic pattern formation. Nature **400,** 687, 1999.
32. Josse, S., Faucheux, C., Soueidan, A., Grimandi, G., Massiot, D., Alonso, B., Janvier, P., Laïb, S., Pilet, P., Gauthier, O., Daculsi, G., Guicheux, J.J., Bujoli, B., and Bouler, J.M. Novel biomaterials for bisphosphonate delivery. Biomaterials **26,** 2073, 2005.
33. Pascaud, P., Errassifi, F., Brouillet, F., Sarda, S., Barroug, A., Legrouri, A., and Rey, C. Adsorption on apatitic calcium phosphates for drug delivery: interaction with bisphosphonate molecules. J Mater Sci Mater Med **25,** 2373, 2014.
34. Chou, J., Ito, T., Bishop, D., Otsuka, M., Ben-Nissan, B., and Milthorpe, B. Controlled release of simvastatin from biomimetic β-TCP drug delivery system. PLoS One **8,** e54676, 2013.
35. Uskoković, V., and Uskoković, D.P. Nanosized hydroxyapatite and other calcium phosphates: chemistry of formation and application as drug and gene delivery agents. J Biomed Mater Res B Appl Biomater **96,** 152, 2011.
36. Barrere, F., van Blitterswijk, C.A., de Groot, K., and Layrolle, P. Influence of ionic strength and carbonate on the Ca-P coating formation from SBFx5 solution. Biomaterials **23,** 1921, 2002.
37. Dong, X., Wang, Q., Wu, T., and Pan, H. Understanding adsorption-desorption dynamics of BMP-2 on hydroxyapatite (001) surface. Biophys J **93**, 750, 2007.

Address correspondence to:
Min Lee, PhD
Division of Advanced Prosthodontics
UCLA School of Dentistry
10833 Le Conte Ave., CHS 23-088F
Los Angeles, CA 90095-1668

E-mail: leemin@ucla.edu

Tara Aghaloo, DDS, MD, PhD
Division of Diagnostic and Surgical Sciences
UCLA School of Dentistry
10833 Le Conte Ave., CHS 53-009
Los Angeles, CA 90095-1668

E-mail: taghaloo@dentistry.ucla.edu

Received: August 14, 2014
Accepted: March 25, 2015
Online Publication Date: May 19, 2015